OPEN ACCESS

Original research

Immunosuppressive contribution of tumour-infiltrating B cells in human intrahepatic cholangiocarcinoma and their role in chemoimmunotherapy outcome

Giulia Milardi,[1] Barbara Franceschini,[1] Chiara Camisaschi,[2] Simone Puccio,[3,4] Guido Costa,[5,6] Cristiana Soldani,[1] Paolo Uva,[7] Davide Cangelosi,[7] Roberta Carriero,[8] Luca Lambroia ,[8] Antonella Cammarota,[1,6] Giulio Lodetti-Zangrandi,[1] Ines Malenica,[4] Marco Erreni,[6,9] Ilaria Montali,[2] Chiara Raggi,[10] Paolo Kunderfranco,[8] Michela Anna Polidoro,[1] Alessio Aghemo,[6,11] Rita Balsano,[6,12] Tiziana Pressiani,[12] Salvatore Piscuoglio,[6,13] Luca Di Tommaso,[6,13] Guido Torzilli,[5,6] Lorenza Rimassa,[6,12] Enrico Lugli,[4] Barbara Cassani,[14,15] Ana Lleo [6,11]

► Additional supplemental material is published online only. To view, please visit the journal online (https://doi.org/10.1136/gutjnl-2025-334861).

For numbered affiliations see end of article.

Correspondence to
Professor Ana Lleo;
ana.lleo@humanitas.it

Received 23 January 2025
Accepted 15 August 2025

To cite: Milardi G, Franceschini B, Camisaschi C, *et al*. *Gut* Epub ahead of print: [*please include* Day Month Year]. doi:10.1136/gutjnl-2025-334861

ABSTRACT

Background Intrahepatic cholangiocarcinoma (iCCA) is a highly aggressive biliary tract cancer with a poor prognosis and a complex tumour microenvironment (TME) that remains poorly understood.

Objective This study aimed to investigate the phenotypic and molecular characteristics of B lymphocytes, their interactions with the TME and their prognostic implications.

Design B-cell compartments in the tumour, peritumour, and peripheral blood of iCCA patients were analysed using multimodal single-cell technologies. The B-cell interactome with the iCCA TME was explored in silico, and ex vivo assays assessed the impact of interactions with cancer-associated fibroblasts (CAFs) and tumour cells on B-cell biology. B-cell modulation during chemoimmunotherapy in advanced iCCA was also evaluated.

Results B cells were enriched in adjacent tumour-free tissues and formed mature tertiary lymphoid structures (TLS), correlating with better prognosis. Conversely, tumour-infiltrating B cells were scarce, immature and displayed reduced effector function with increased immunosuppressive features. Coculture with tumour cells or CAFs impaired B-cell differentiation and function, including downregulation of BAFFR in peripheral B cells. IL-6 and TGF-β emerged as major drivers of B-cell dysfunction; dual blockade restored B-cell activation and differentiation. Elevated frequencies of circulating BAFFR^{+} B cells and hyperexpanded clonotypes were linked to improved chemoimmunotherapy response.

Conclusions iCCA is characterised by a profoundly immunosuppressive TME that impairs B-cell function through soluble factors and cellular interactions. Our findings identify B cells as biomarkers and therapeutic targets, supporting strategies to restore B-cell function and promote mature TLS to enhance immunotherapy responsiveness in iCCA.

WHAT IS ALREADY KNOWN ON THIS TOPIC

⇒ Intrahepatic cholangiocarcinoma (iCCA) is a highly aggressive malignancy with poor prognosis and limited treatment options.
⇒ A chronically inflamed and immunosuppressive tumour microenvironment (TME) contributes to iCCA progression, poor outcomes and resistance to immunotherapy.
⇒ The role of B lymphocytes in the iCCA microenvironment remains poorly understood and has been largely overlooked.

INTRODUCTION

Intrahepatic cholangiocarcinoma (iCCA) is a rare and aggressive biliary tract cancer with an increasing global incidence and poor outcomes. Surgery remains the only potentially curative treatment; however, the combination of immunotherapy and chemotherapy has been shown to improve survival, leading to its approval as the preferred first-line treatment for advanced iCCA.[1 2]

iCCA develops in a complex and highly desmoplastic tumour microenvironment (TME) influenced by cancer-associated fibroblasts (CAFs), extracellular matrix (ECM) and immune cells, which support tumour progression.[3 4] Transcriptomic analyses revealed that tumour-infiltrating lymphocytes (TILs) play a key role in immune evasion and treatment responses.[5–8] Recent genomics, molecular and immune characterisations of the TME have led to the classification of iCCA into immune-desert, immune-activated, myeloid-enriched and mesenchymal-like subsets.[9]

B cells are key players in adaptive immunity, with their development guided by genetic factors and environmental signals.[10] In the context of tumours, B cells may promote tumour growth by supporting regulatory B cells and suppressing immune responses.[11] Conversely, B cells can also fight tumours by producing specific antibodies and cytokines that enhance the activity of T cells,

WHAT THIS STUDY ADDS

⇒ High densities of B cells in peritumoural areas and their organisation into mature tertiary lymphoid structures are associated with favourable prognosis.
⇒ B cells infiltrating iCCA tumours are predominantly immature and functionally suppressed.
⇒ Primary tumour cells and cancer-associated fibroblasts drive B-cell dysfunction by promoting IL-6-dependent and TGF-βdependent immunosuppressive pathways.
⇒ BAFFR+ B cells in peripheral blood predict response to chemoimmunotherapy.

HOW THIS STUDY MIGHT AFFECT RESEARCH, PRACTICE OR POLICY

⇒ This work expands the immunological understanding of iCCA, highlighting the interplay between immune and stromal elements of the TME as key regulators of tumour immunity.
⇒ Targeting B-cell–TME interactions, particularly via IL-6 and TGF-β blockade, may offer novel therapeutic avenues to restore B-cell function and enhance immunotherapy efficacy.
⇒ B-cell phenotypes, including BAFFR+ subsets, may serve as prognostic and predictive biomarkers, informing future stratification strategies and immunotherapeutic approaches in iCCA.

macrophages and NK cells.[12–17] Further, tumour-infiltrating B lymphocytes (TIL-B) are involved in forming and maintaining tertiary lymphoid structures (TLSs), sites for local immune responses and antibody maturation.[13 18–20] Finally, TIL-B shows strong potential as predictive and prognostic markers for treatment with immune checkpoint inhibitors (ICIs).[21]

This study aims to dissect the role of B lymphocytes in iCCA by examining their nature and function. This could reveal new mechanisms of cancer progression or control and help identify biomarkers for predicting responses to ICIs.

MATERIALS AND METHODS

Study design and sample collection

Patient and public involvement

Patients were not involved in the design of the study, nor in the recruitment and conduction of the study. All patients had pathology-confirmed iCCA, without targetable mutations, and were treatment naïve prior to surgical resection. Patients with viral hepatitis and those with cirrhosis were excluded. Tissue samples were collected from areas without visible necrosis or haemorrhage. The 2 μm formalin-fixed and paraffin-embedded tissue sections were stained with H&E and evaluated by a liver pathologist (laboratory developed tests, LDT). Estimated features included tumour grade, desmoplasia, resection margins, steatosis, perineural and lymphovascular invasion, and lymph node metastasis. Patients with resected iCCA were monitored every 3 months or until death, with major events recorded. Patients with advanced iCCA received chemoimmunotherapy (durvalumab, cisplatin and gemcitabine); tumour assessments were conducted every 8 weeks starting from baseline.[22 23] Characteristics of the enrolled patients are listed in online supplemental table 1.

Peripheral blood mononuclear cells (PBMCs) were isolated from buffy coats from iCCA and healthy donors (HDs) via density-gradient separation and were cryopreserved in fetal bovine serum (FBS) supplemented with 10% dimethyl sulfoxide (DMSO) until use. Tissues were collected and stored as previously described.[8]

Polychromatic flow cytometry

Single-cell suspensions were first stained with Zombie Aqua fluorescent dye (BioLegend) to eliminate dead cells. Cell pellets were incubated with a combination of monoclonal antibodies, selected based on current knowledge[12 24 25] and listed in online supplemental table 2. We followed the flow cytometry procedures previously described[26 27] for (1) selection of antigen-fluorochrome combinations, (2) reagent titration and validation and (3) limiting spreading error. Stained samples were analysed using a FACS-Symphony A5 cytometer (BD Biosciences). Compensation was done using BD Compbeads incubated with single antibodies (BD Biosciences). FlowJo V.10.8.1 was used for the gating analysis (online supplemental figure 2). Additional methods are provided in the online supplemental file 2 and online supplemental tables 3–7.

RESULTS

Prognostic value of B cells and TLSs in iCCA

We initially performed immunohistochemical analysis on tumour and peritumoural tissues from resected iCCA patients (n=103), stratifying samples based on $CD20^+$ B cell density. A threshold of 30% B cells out of total TILs was used to define 'high' and 'low' B cell content. High B cell infiltration in the peritumoural area was significantly associated with improved disease-free survival (DFS) (p=0.0245; figure 1A), suggesting a potential protective role of B cells in this compartment. Conversely, intratumoural B cell content showed no association with DFS (p=0.6922; figure 1B), likely reflecting their lower abundance in the tumour core and the presence of a more immunosuppressive microenvironment, which may impair B cell function. Single and dual immunohistochemistry (anti-CD3 and anti-CD20) analysis revealed that, in 49.51% of patients, B lymphocytes were organised in cellular aggregates morphologically like TLSs, which contained mainly $CD3^+$ T cells encircling an inner population of $CD20^+$ B cells (figure 1C). Notably, these structures were identified both in the peritumoural area and within the tumour tissue (figure 1C). TLS maturation stages were classified according to the distribution of $CD3^+$ T cells, in early or immature (iTLSs) and mature (primary and secondary follicle) (mature TLS, mTLSs).[28 29] While iTLSs contain dispersed $CD3^+$ T cells, mTLSs are characterised by a tight cell core.[30] Based on these criteria, we explored the prognostic value of TLS-related features in iCCA (figure 1D). To estimate the relative abundance of TLS for each specimen, the absolute number of iTLS and mTLS was normalised by the total number of TLS. Similarly to other tumours,[31] the presence of mTLS (≥75% of total TLS) showed positive prognostic significance (figure 1E, p-values=0.0388).

scRNA-seq reveals tumour-specific differences in gene expression by B-cell subpopulations

We next took advantage of our previously described transcriptional profile of $CD45^+$ cells, isolated from iCCA samples and adjacent normal tissue,[8] to define the molecular signature of B cells within the iCCA TME. After extracting all B cells (using the expression of marker genes *CD79A*, *MS4A1*)[32] for further subclustering analysis, four main clusters were reliably identified (figure 2A,B), annotated as previously reported by Monaco.[33] Cluster C0 of naïve B cells exhibited high expression levels of genes involved in B cell receptor signalling and trafficking pathways (*RGS1*, *CD79B*, *IGHD*, *BLNK*, *IL4R* and *LY9*); cluster

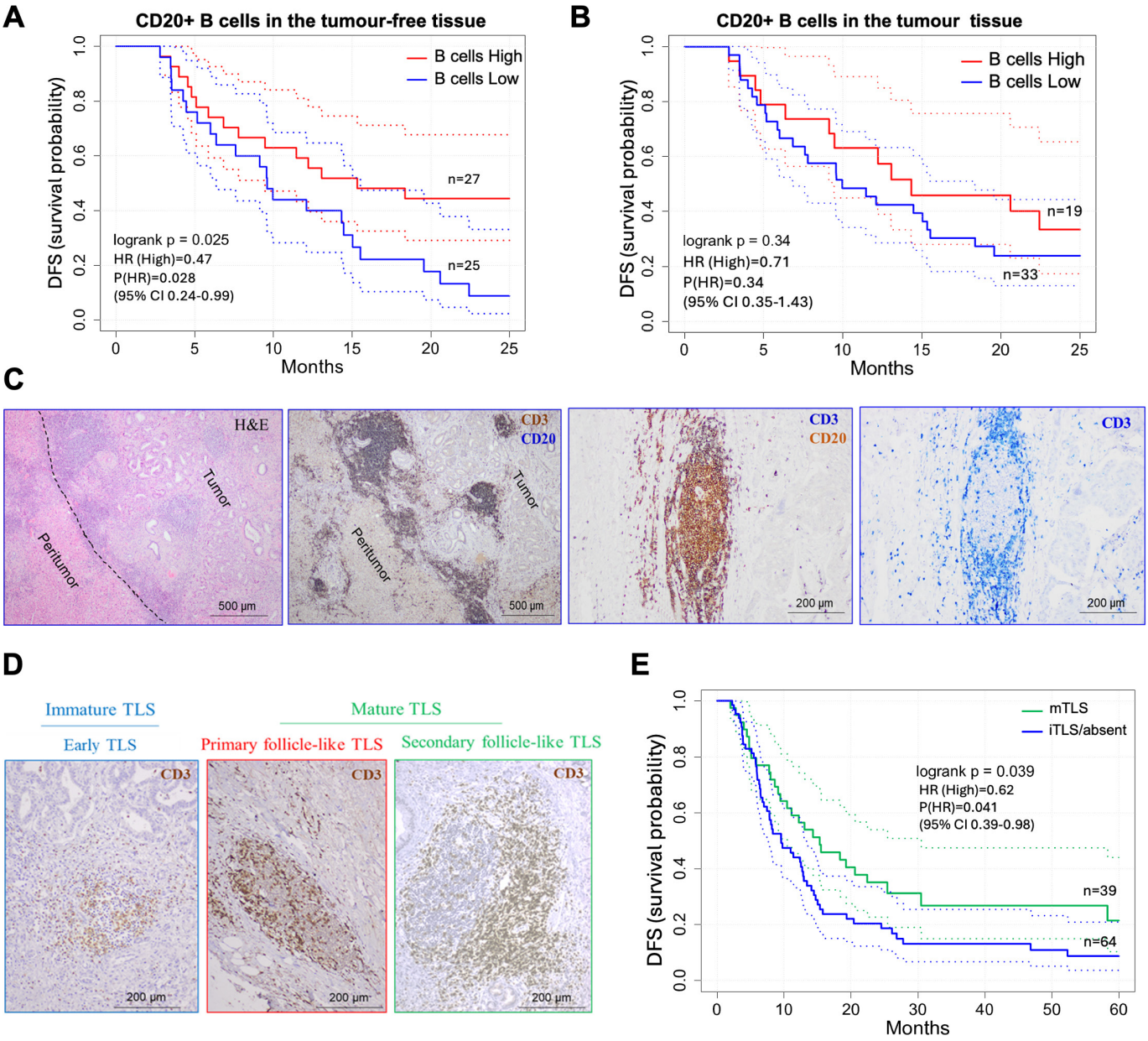

Figure 1 B cell enrichment in peritumoural areas and presence of mTLS are associated with improved prognosis in iCCA. (A, B) Kaplan-Meier DFS curves comparing iCCA patients (n=39) stratified by high (≥30%) vs low (<30%) density of CD20$^+$ B lymphocytes in peritumoural (A) and intratumoural (B) regions, as assessed by IHC. (C) Representative FFPE tissue sections showing CD3$^+$ T cells and CD20$^+$ B cells organised into TLS located either within or outside the tumour area. TLS were classified based on cellular composition and spatial organisation. (D) IHC images highlighting TLS maturation stages, from iTLS lacking clear compartmentalisation, to mTLS with distinct B and T cell zones. CD3$^+$ T cells surround CD20$^+$ B cell clusters, reflecting follicle-like architecture. (E) Kaplan-Meier DFS analysis of a larger iCCA cohort (n=103), comparing patients with absent or iTLS to those with mTLS, defined by the presence of primary or secondary follicle-like structures. DFS, disease-free survival; FFPE, formalin-fixed paraffin-embedded; iCCA, intrahepatic cholangiocarcinoma; IHC, immunohistochemistry; iTLS, immature TLS; mTLS, mature TLS; TLS, tertiary lymphoid structures.

C1 of switched memory/exhausted B cells highly expressed the activation-related genes (*S100A10*, *PLP2*, *IGHM*, *CD44*, *IGHA1*, *PKM*, *LDHB*, *ANXA2* and *LGALS1*); cluster C2 of non-switched memory B cells displayed high expression levels of many proteins associated to stress responses (*HSPA6*, *HSPE1*, *HSPB1*, *HSPA1A* and *UBC*) and *CD69*; cluster C3 was characterised by prominent expression of markers normally associated with T cells (*IL7R*, *NKG7*, *CD2*, *CD3e*, *ANXA1*, *KLRB1*, *CD7* and *IL-32*) (figure 2B). Gene set enrichment analysis (GSEA) on bona fide B cell clusters further confirmed that C0 was characterised by gene set and transcription factors associated with the resting and metabolically quiescent naive state; C1 was characterised by transcripts associated with fatty acid metabolism and oxidative phosphorylation; whereas C2 was characterised by transcripts associated with stress response under hypoxia and inflammation (figure 2, online supplemental figure 1A, online supplemental file 3). Cluster analysis of scRNA-seq data revealed that the tumour area was poorly enriched with B cells and each B cell cluster was less abundant within the tumour compared with non-tumoural tissues (figure 2D), in agreement with the poorly immunogenic nature of iCCA.

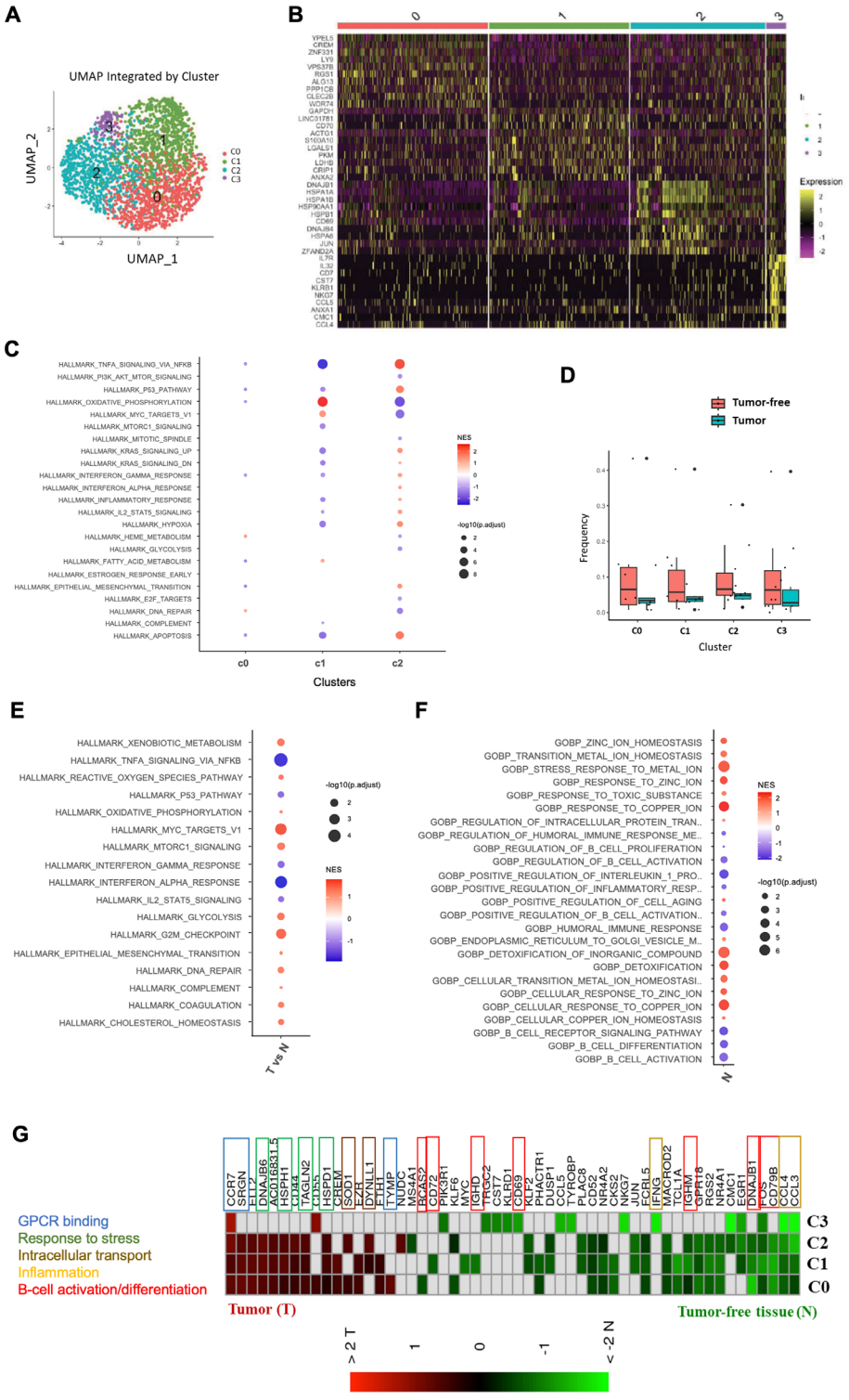

Figure 2 Transcriptome of infiltrating B lymphocytes in iCCA tumours and adjacent tissue reveals heterogeneity of B cells in iCCA. (A) UMAP plot from scRNA-seq of paired tumour and adjacent non-tumour liver tissues from six treatment-naïve iCCA patients, showing four distinct B cell clusters: C0 (naïve B cells), C1 (switched memory/exhausted B cells), C2 (non-switched memory B cells) and C3 ($CD3^{+}CD20^{+}$ double-positive cells). (B) Heatmap displaying expression of top marker genes for each B cell cluster. Columns represent single cells, and rows correspond to cluster-defining genes. (C) GSEA comparing hallmark gene sets across B cell clusters (adjusted p<0.05). Enrichment is shown as NES. (D) Relative frequency distribution of each B cell cluster in tumour versus adjacent non-tumour tissue. Each point represents an individual sample; lines indicate median values. (E) GSEA pseudo-bulk analysis highlighting hallmark pathways differentially expressed in tumour versus non-tumour samples within clusters C0, C1 and C2. NES indicates direction and strength of enrichment. (F) GSEA pseudo-bulk analysis of Gene Ontology Biological Processes (GO-BP) for differentially expressed genes in tumour versus non-tumour samples, stratified by B cell cluster. (G) Volcano plot of differentially expressed genes between tumour and adjacent non-tumourous tissue across all B cells. Genes with adjusted p<0.05 are shown. GO-BP, Gene Ontology Biological Process; GSEA, Gene Set Enrichment Analysis; iCCA, intrahepatic cholangiocarcinoma; NES, normalised enrichment score; UMAP, Uniform Manifold Approximation and Projection.

We then used GSEA to screen out valuable hallmark gene sets for tumourous compared with peritumoural tissues. We found that G2M checkpoint, DNA repair, MYC targets, glycolysis and xenobiotic metabolism were abnormal hallmark gene sets in tumour tissue versus adjacent normal tissue, whereas inflammatory pathways were strongly downregulated (figure 2E). Remarkably, in-depth GSEA analysis of biological process and pathways further unveiled that BCR signalling, B cell differentiation and humoral responses were markedly suppressed in the tumour (figure 2F, online supplemental figure 1B,C, online supplemental file 3). In agreement, several B cell activation/differentiation genes (*MS4A1, CD72, MYC, CD69, TCL1A, eg,R1, FOS, CD79B, JUN, RGS2, CD52*) and those involved in inflammation (*INF-γ, CCL4, CCL3*) were downregulated in iCCA tumour compared with adjacent non-tumour tissue (figure 2G). On the contrary, intratumoural B cells showed an upregulation of genes involved in cellular stress response (*DNAJB6, HSPH1, TAGLN2, HSPD1*) and GPCR binding (*CCR7, SRGN, TYMP*) (figure 2G). Overall, these data highlight not only the poor B cell infiltration of iCCA but also the functional impairment of intratumoural B cells.

High-dimensional flow cytometry defines the B-cell composition of human iCCA

We next developed a polychromatic flow cytometry panel and characterised single B cell suspensions from resected tumour, paired adjacent cancer-free tissue (peritumour), distal tumour-free tissue, intrahepatic blood (perfusate) and peripheral blood (PB) of 19 treatment-naïve surgically resected patients (figure 3A). The panel was designed to examine markers of B cell differentiation, maturation and activation (online supplemental table 2), results were analysed using PhenoGraph.[34 35] Specifically, we identified 15 putative B cell subpopulations (figure 3B), whose profile of antigen expression is shown in figure 3A. Data analysis revealed a substantial difference of $CD19^+$ B cell clustering profile between the two main districts (blood vs tissue) (figure 3C, online supplemental figure 3B,C, online supplemental file 3). Specifically, clusters of memory B cells were particularly present in the PB and perfusate, including activated, $CD27^+IgD^+IgM^+$ unswitched (NSM), $CD27^+IgD^-$ switched (SM) and IgA^+ memory B cells (figure 3, online supplemental figure 3C,D, online supplemental file 3). On the other hand, tissue samples were predominantly enriched in the subsets of $CD27^-IgD^+$ naïve as well as atypical and double negative B cells, identified as $CD27^-IgD^-$ (DN1,2,3), expressing low levels of activation markers. Within the tumour, clusters of $CD24^-CD21^-CD27^-IgD^-$ double negative 2 B cells (characterised by high expression of activation markers HLA-DR, PD1) (C9), $CD38^+CD24^+CD10^+$ immature (C13), $CD27^-IgD^+IgM^+$ marginal zone naïve B cells (C12) and $CD38^+CD20^-$ plasmablasts (C11) (figure 3D, online supplemental figure 3D, online supplemental file 3) were shown to be reduced, confirming that the tumour is largely devoid of TIL-B populations promoting antitumour immunity. In contrast, no significant differences were observed for memory and mature naïve B cell subsets. This finding suggests a selective depletion or dysfunction of antigen-responsive B cell populations in the tumour milieu, potentially reflecting their higher sensitivity to immunosuppressive cues.[36]

Finally, tissue samples were overall characterised by lower frequencies of B cells expressing key markers associated with B-cell differentiation and maturation, including BAFF-receptor (BAFFR), CD21 and CD44; whereas they displayed higher liver markers associated with tissue-residency, such as CD69 and CD70 (figure 3E, online supplemental figure 3E, online supplemental file 3).

Ex vivo functionality of B cells revealed impaired immunoglobulin isotype production and a regulatory phenotype within the tumour tissue

To investigate the functional consequences of the observed B cell phenotype, we quantified the Ig isotypes in the plasma of patients with iCCA (n=26). Patients displayed remarkably lower IgM, IgG2, IgG4, IgA and IgE concentrations compared with HD (figure 4A). Interestingly, levels of IgG1 and IgG3, which have a high capacity to trigger antibody-dependent cellular cytotoxicity and activate the complement cascade,[37] maintained normal levels (figure 4A). As IgG1 and IgG3 are products of early class-switch recombination (CSR), their selective preservation, alongside the loss of later isotypes, suggests a block in CSR progression. This is consistent with the downregulation of key differentiation markers observed in tumour-associated B cells, pointing to impaired B cell maturation and a defective humoral immune response in iCCA.

We next performed a comparative analysis of B cells sorted from tumour and tumour-free adjacent tissues and showed that TIL-B express higher levels of immunosuppressive cytokines (IL-10 and TGFβ) (figure 4B) and lower levels of proinflammatory cytokines (IL-6 and IL-12), typical of effector B cell populations, compared with the tumour-free tissue (figure 4B). TIL-B also upregulated TNF-α, a critical tumour promoter able to enhance the immunosuppressive capacity of Tregs.[38] These data suggest that TIL-B may develop into a regulatory phenotype and could thereby sustain the immunosuppression when present in the iCCA microenvironment.

Molecular characterisation of B cell interactome in iCCA microenvironment

We next analysed TIL-B interactions with the surrounding microenvironment by using CellPhoneDB (online supplemental methods) and taking advantage of a public scRNA-seq dataset of iCCA (HRA000863).[39] We found that B cells establish connections with both CAFs and tumour cells (online supplemental figure 4A, online supplemental file 3), engaging pathways linked to inflammation, negative regulation of immune cell activation, proliferation, development and effector function, cytokine signalling and lymphoid structure formation (online supplemental figure 4B,C, online supplemental file 3). The interactions with CAFs involve a variety of ligand-receptor pairs (online supplemental figure 4D,E, online supplemental file 3), including interactions with a specific subset of antigen-presenting CAFs expressing high levels of HLA-related genes[40] (online supplemental figure 4D, online supplemental file 3). Importantly, enhanced predicted interaction between *CXCL12*, *CCL4*, *LTBR* expressed by CAFs and *CXCR4*, *CNR2*, *LTB*, respectively, on B cells suggests a role in B cell homing/retention and lymphoid structure formation.[41] Additionally, B cells engage with CAFs through *CD74–MIF/APP/COPA*, which regulates survival and proliferation and is highly expressed during tumour progression[42]; and *CD40/BAFF* receptor (*TNFRSF13C*)*–BAFF* (*TNFSF13B*) involved in TGFβ production and liver fibrosis.[43] Finally, CD55+B cells, associated with immune-suppressive features, interact with *ADGRE5* on CAFs. Importantly, *CD55* was identified as a differentially expressed gene in TIL-B (figure 2G) linked to immune-suppressive functions and tumour immune evasion.[44] We also observed that *CD44–FGFR2* and *TGFB1* interactions mediate communication between B cells and

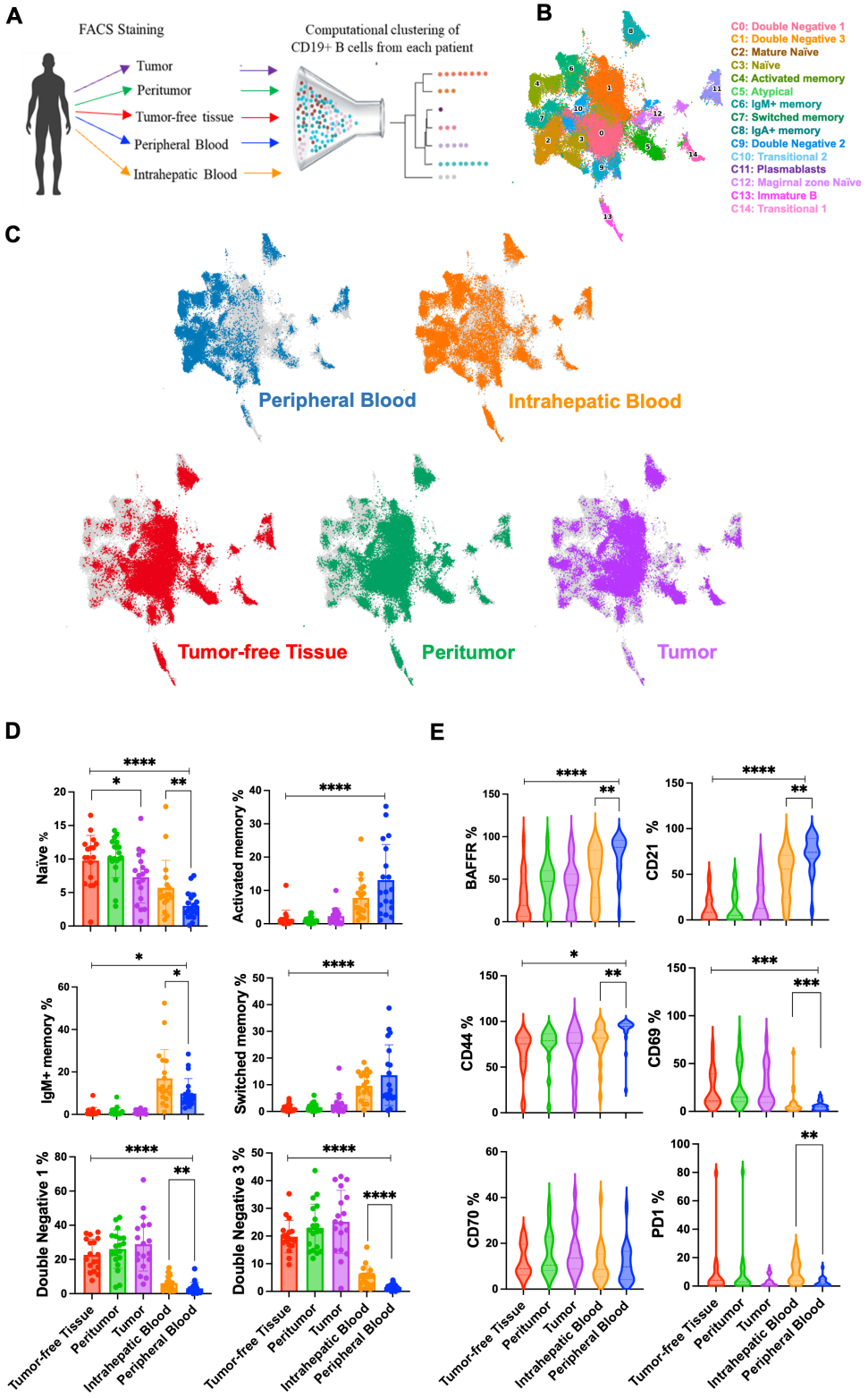

Figure 3 High-dimensional flow cytometry reveals B cell heterogeneity, distribution and activation states in iCCA. (A) Schematic representation of the experimental workflow. B cells were isolated from tumour (T), peritumoural (PT), tumour-free liver (NT), PB and IHB of iCCA patients and analysed by high-parameter flow cytometry. (B) UMAP of PhenoGraph clustering, identifying 15 B cell populations from pooled samples (n=19 patients), based on expression of surface markers. (C) UMAP coloured by tissue origin, showing the distribution of B cell subsets across NT, PT, T, PB and IHB compartments. (D) Quantification of B cell subset frequencies—including naïve ($CD19^+CD27^-IgD^+$), activated, unswitched memory ($CD19^+CD27^+IgD^+$), switched memory ($CD19^+CD27^+IgD^-$) and double-negative ($CD19^+CD27^-IgD^-$) B cells—across different anatomical sites. (E) Percentages of total B cells expressing key activation, differentiation and maturation markers (eg, BAFFR, CD44, CD38, PD1, CD71) in the same tissue compartments. Data are derived from >10 independent experiments (iCCA n=19). Each dot represents one patient sample; bars indicate SD. Statistical comparisons were made using the Mann-Whitney or ANOVA tests. *p<0.05; **p<0.005; ***p<0.001; ****p<0.0001. ANOVA, analysis of variance; iCCA, intrahepatic cholangiocarcinoma; IHB, intrahepatic blood; PB, peripheral blood.

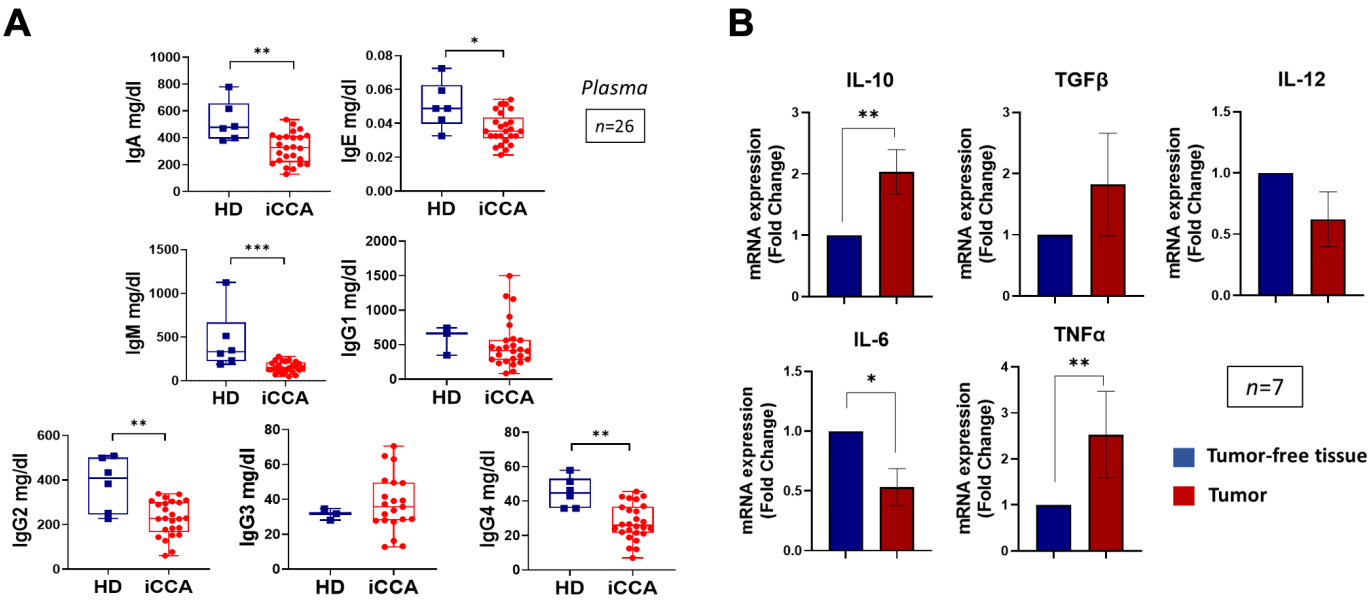

Figure 4 Impaired systemic immunoglobulin levels and altered cytokine gene expression in intratumoural B cells from iCCA patients. (A) Quantification of circulating immunoglobulin isotypes (IgG, IgA, IgM, IgE) in plasma from patients with intrahepatic cholangiocarcinoma (iCCA, n=26) and (HD, n=10), measured by multiplex bead-based immunoassay. Values are reported in mg/dL. (B) Quantitative RT-PCR analysis of immunoregulatory cytokine transcripts (eg, IL-10, IL-6, TGF-β1) in intratumoural versus tumour-free $CD19^+CD20^+$ B cells, FACS-purified from iCCA tissue samples (n=7 patients). Expression levels are shown as fold change relative to matched non-malignant tissue. Bars indicate SD; each dot represents one individual patient. Statistical analysis performed using Mann-Whitney U test. *p<0.05; **p<0.005; ***p<0.001. FACS, fluorescence-activated cell sorting; HD, healthy donor; iCCA, intrahepatic cholangiocarcinoma.

tumour cells, with *CD44* being upregulated in all TIL-B subsets (figure 2G). The *LGALS9* ligand-receptor pair was enriched in interactions between B cells and tumour cells, indicating a potential role for tumour cells in inhibiting B-cell activation.[45] Further analysis of B cell subpopulations in public scRNA-seq (HRA000863)[39] revealed four main clusters, confirming our previous analysis (figure 5A–C, online supplemental figure 4F, online supplemental file 3). All B cell subpopulations interacted with CAFs and tumour cells, with non-switched memory B cells (C2) exhibiting the highest number of predicted cellular interactions (n=58 with CAFs; n=56 iCCA cells). Overall, these findings imply that TIL-B in iCCA engage in cell–cell communication with TME receptor-ligand pairs, potentially influencing their activation and promoting immune-regulatory functions.

We further used high-dimensional tissue mass cytometry to analyse the spatial distribution of B cells in tumour tissue. The selected antibodies to identify different cell types included tumour epithelial cells (E-cadherin+), stromal cells (α-SMA^+), B cells ($CD45^+CD20^+$), T cells ($CD45^+CD3^+$) and endothelial cells ($CD31^+$) (figure 5D, online supplemental figure 5, online supplemental file 3). The analysis revealed that B cells, whether organised in TLS or not, were mainly located at the invasive front of the tumour, close to tumour nests and in stromal areas (figure 5D, online supplemental figure 5, online supplemental file 3), suggesting that CAFs and the ECM may act as a barrier to leucocyte migration.[46]

ICCA cells and CAFs affect B cell polarisation and activation state

To validate the interactions between TIL-B, tumour cells and CAFs, we conducted ex vivo coculture experiments. Human primary iCCA cells and CAFs isolated from resected tumour specimens (online supplemental figure 6A,B, online supplemental table 6) were cocultured with $CD19^+CD27^-IgD^+$ naïve B cells FACS-sorted from the PB of HDs (figure 5E). FACS analysis after 6 days of coculture showed a low frequency of switched and unswitched memory B cells, mature naïve B cells and plasmablasts. This was accompanied by an increase in double-negative and atypical B cell subsets, resembling the B cell phenotypes found in ex vivo analyses of iCCA TIL-B (online supplemental figure 5F–7A, online supplemental file 3). This effect was more pronounced when B cells were co-cultured with tumour cells (online supplemental figure 5F–7A, online supplemental file 3). Additionally, the percentage of naïve B cells expressing activation and maturation markers (ie, BAFFR, PD1, CD21, CD40, CD70, CD69, ICOSL and CD44) was significantly reduced compared with the control if cultured with CAFs or tumour cells (online supplemental figure 5A–7B, online supplemental file 3).

Further, FACS analysis revealed that B cells cocultured on a transwell system with iCCA cells exhibited impaired differentiation capabilities (online supplemental figure 8A, online supplemental file 3). While naïve B cells still showed some ability to differentiate into an unswitched memory phenotype, their transition to switched memory B cells was notably diminished (online supplemental figure 8B, online supplemental file 3). We also observed a significant increase in atypical B cells and a decrease in activated B cells and plasmablasts compared with controls (online supplemental figure 8B, online supplemental file 3). The frequency of B cells expressing activation markers (including BAFFR, PD1, CD44, CD70 and CD69) decreased when cocultured with tumour cells, suggesting that CAFs have a lesser role in influencing the effector phenotype of B cells through crosstalk (online supplemental figure 8C, online supplemental file 3). Real-time PCR confirmed the upregulation of both immunoregulatory (IL-10 and TGFβ) and proinflammatory factors (IL-12, IL-6 and TNFα) in naïve B cells cocultured with tumour cells, highlighting their role in modulating B cell immune responses, while minor differences were noted

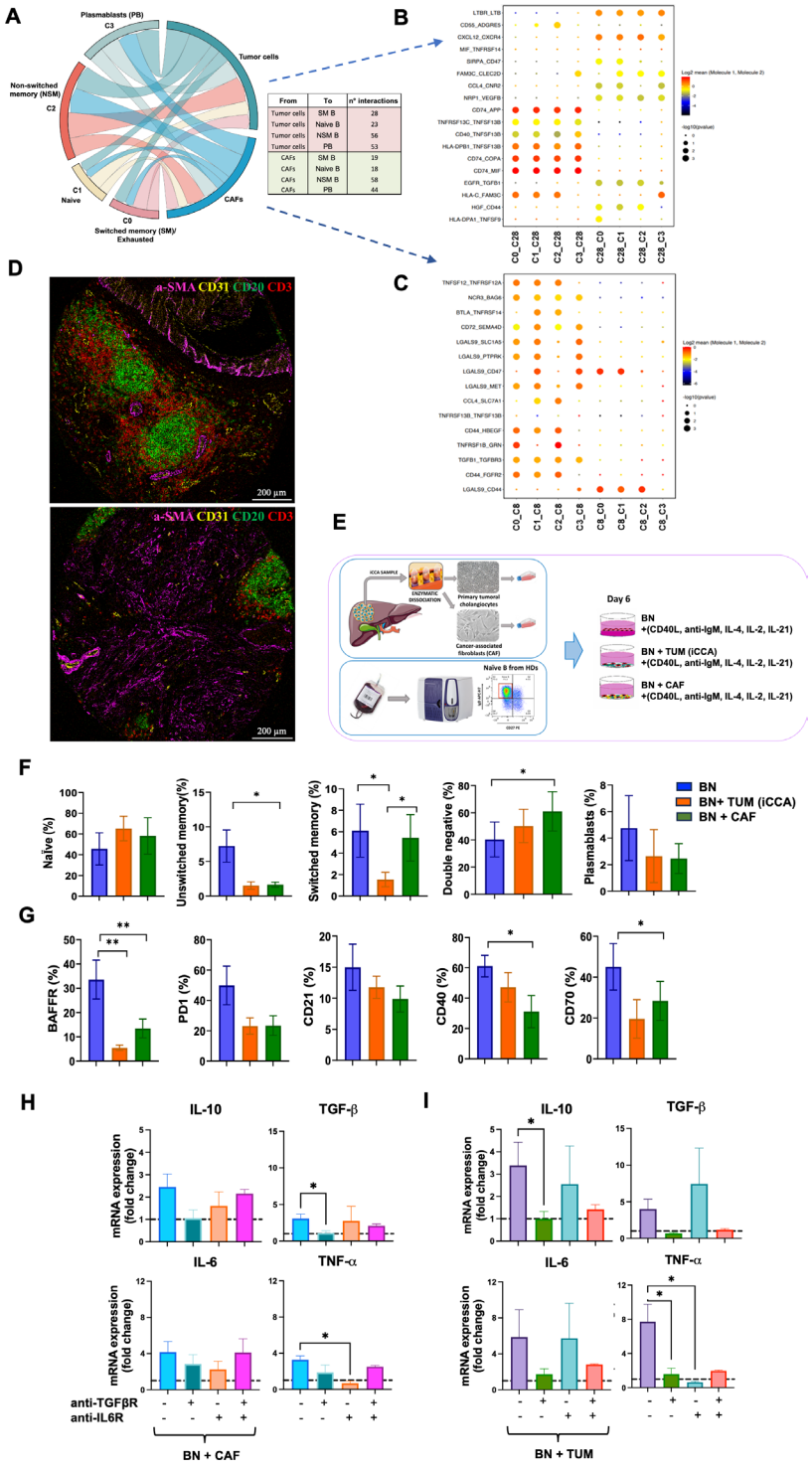

Figure 5 Molecular and functional characterisation of B cell interactions with tumour cells and CAFs in iCCA. (A) CellPhoneDB-based analysis of ligand–receptor interactions between B cell subsets and either CAFs (cluster 28) or tumour epithelial cells (cluster 8), using a public single-cell RNA-sequencing (scRNA-seq) dataset from iCCA patients. (B, C) Circos plots showing predicted ligand–receptor (L:R) interactions between CAFs (B) or tumour cells (C) and B cell subsets. Bubble plots indicate mean expression of each L:R pair (colour scale) and interaction significance (bubble size based on p value). (D) Imaging mass cytometry of a representative iCCA sample showing a TLS with co-localised immune and stromal markers. (E) Schematic of the experimental setup for co-cultures of naïve B cells with primary iCCA tumour cells or CAFs, using both direct and transwell systems. (F) Flow cytometry analysis of B cell subset distribution following 6 days of direct co-culture with iCCA cells or CAFs (n=5 independent patients). Subsets include naïve, memory and double-negative B cells. (G) Frequency of B cells expressing key markers of differentiation (eg, CD27), activation (eg, BAFFR), and exhaustion (eg, PD-1, CD70) after co-culture. (H, I) Quantitative RT-PCR analysis of cytokine transcripts (eg, IL-10, IL-6, TGF-β1) in B cells after 6 days of co-culture in transwell systems between healthy donor naïve B cells and CAFs (H) or primary iCCA cells (I), with or without treatment with anti-IL-6 (tocilizumab), anti-TGF-β, or their combination; expressed as fold change vs control naïve B cells. Bars indicate SD. Statistical significance assessed using Mann-Whitney U and one-way ANOVA tests. *p<0.05; **p<0.005. ANOVA, analysis of variance; CAFs, cancer-associated fibroblasts; iCCA, intrahepatic cholangiocarcinoma; TLS, tertiary lymphoid structure.

when B cells were cocultured with CAFs (online supplemental figure 8D, online supplemental file 3). Cytokine concentration in the basolateral supernatant after 6 days of coculture showed a significant increase in IL-10 and pro-inflammatory cytokines (IL-6 and IL-12p70) in cultures with either iCCA cells or CAFs. Conversely, when naïve B cells were cultured with tumour cells, the production of other inflammatory factors (eg, IL-13, TNF-α, TNF-β, INF-γ, IL-17A) decreased, while the addition of CAFs did not significantly affect the levels of these cytokines (online supplemental figure 9, online supplemental file 3).

To investigate the mechanisms underlying B cell dysfunction in iCCA, we leveraged our previously performed interactome analysis between B cells and components of the TME, which identified TGF-β and IL-6 as prominent immunosuppressive signals potentially mediating B cell–tumour crosstalk. Consistently, ELISA confirmed that both iCCA cells and CAFs secrete high levels of these cytokines (online supplemental figure 10A, online supplemental file 3). Based on these observations, we inhibited TGF-βR1/2 (LY2109761) and IL-6R (tocilizumab) in transwell cocultures with naïve B cells. Cytokine blockade, particularly the dual inhibition, restored B cell activation and differentiation, as shown by increased expression of BAFFR, CD40, CD44, CD69 and PD1, and expansion of memory B cells and plasmablasts (online supplemental figure 10B,C, online supplemental file 3). Quantitative RT-PCR analysis revealed that combined blockade significantly reduced expression of both immunoregulatory (IL-10, TGF-β) and pro-inflammatory (IL-6, TNF-α) cytokines in B cells, with the strongest effect observed in cocultures with tumour cells (figure 5H,I). These findings indicate that TGF-β and IL-6 synergistically shape a dysfunctional B cell phenotype and that targeting these pathways may restore B cell effector functions within the iCCA microenvironment.

Single-cell phenotypic profiling of circulating B cells in patients treated with ICIs

Finally, we profiled B cells from PBMC collected from 21 patients with advanced iCCA treated with first-line durvalumab-gemcitabine-cisplatin.[47] Eligible patients were classified into responders (n=10, 47.61%) or not-responders (NR, n=11, 52.38%), based on their disease status after 6 months[22 23]; responders included complete response (CR), partial response (PR) and stable disease (SD) (CR: n=1, 4.76%, PR: n=4, 19.05%; SD: n=5, 23.80%), while NR had disease progression.[21 22]

Unsupervised clustering of circulating $CD3^{-}CD19^{+}$ cells confirmed the presence of nine B cell subpopulations (figure 6A,B). Although B cell subsets had a similar distribution in both groups, responders exhibited a higher percentage of B cells expressing key B-cell activation and differentiation markers, that is, BAFFR, CD40, HLA-DR and CD21,[48] compared with NR (figure 6B, online supplemental figure 10A–C, online supplemental file 3). On the other hand, NR showed increased frequencies of CD70+B cells (figure 6B, online supplemental figure 10C, online supplemental file 3), linked to cell exhaustion.[49] Differences in BAFFR and CD70 expression at baseline suggested that these markers could be predictive of therapy outcome. Indeed, Kaplan-Meier analysis revealed that higher BAFFR expression on circulating B cells was associated with better survival (figure 6E, OS: p=0.0016 and progression-free survival (PFS): p=0.0025). Given BAFF's role in the proliferation and maturation of B cells,[50] we quantified BAFF protein levels in the plasma of patients showing higher concentrations in responders both at baseline and at the end of treatment (figure 6F).

To explore B cell clonal dynamics, we performed bulk BCR sequencing at baseline and at cycle 2 day 1 (C2D1) in a subset of eight patients (five responders, three NR). Given that B cells involved in antigen recognition are expected to undergo clonal expansion, we focused on hyperexpanded clonotypes. To minimise confounding effects from pre-existing clonal expansions, our analysis was restricted to hyperexpanded clonotypes identified at C2D1 that were shared by at least two patients. Longitudinal tracking revealed that these treatment-emergent, shared hyperexpanded clonotypes were significantly more abundant in responders compared with NR (online supplemental figure 6G–11D, online supplemental file 3). This suggests that B cell clonal expansion is driven by treatment exposure, occurs early during therapy and is associated with clinical response.

DISCUSSION

In this study, we provide, for the first time, a detailed characterisation of the B cell landscape and function in iCCA and their interactions within the TME; we further show a potential predictive role of B cells in patient response to chemoimmunotherapy in advanced iCCA.

Particularly, our data demonstrate that the iCCA TME is characterised by an immunosuppressive B cell phenotype, highlighted by the downregulation of transcripts related to B cell effector functions and inflammation.[51] Consistently, single-cell immune phenotyping identifies 15 different B cell subsets with a predominance of immature B cells within the tumour compartment and few memory B cells and plasmablasts, indicating a limited capacity to potentially contribute to the antitumour response. The differential distribution of B cell subsets between tumour and peritumoural regions may reflect distinct sensitivities to the TME. Immature and DN2 B cells, which are typically enriched during active immune responses, appear to be preferentially depleted in the tumour, likely due to their dependence on antigenic stimulation and susceptibility to suppression. In contrast, the persistence of memory and mature naïve B cells may reflect a more quiescent or clonally restricted population, possibly maintained by local stromal niches, as described in other tumours.[52] However, the mere presence of these subsets does not equate to function, as they may lack proper activation signals. Circulating B cells mirrored this dysfunction, with impaired immunoglobulin production and receptor signalling.[53 54] Notably, increased frequencies of double-suggest premature exhaustion, as reported in other cancers.[21 36] These cells, typically rare in healthy individuals, might be key in disease progression.[55] TIL-B also displayed reduced expression of BAFFR, CD44 and PD1, consistent with a suppressed state influenced by the TME.[56 57] While phenotypic differences between tumour and peritumoural B cells appeared limited by flow cytometry, single-cell transcriptomics revealed functional divergences, suggesting that qualitative changes, beyond mere cell abundance, may critically shape B cell activity within the iCCA microenvironment.

Building on previous work,[9] we show that both primary tumour cells and CAFs profoundly impair B cell maturation, promoting the expansion of dysfunctional subsets, such as double-negative and atypical B cells, and induce immunosuppressive cytokines, that is, IL-10, TGF-β and IL-6.[58 59] Transcriptomic analyses revealed ligand–receptor interactions between B cells and tumour/CAF compartments, pointing to both contact-dependent and soluble factor-mediated mechanisms.[58] Among the top-ranked immunosuppressive signals, TGF-β and IL-6 emerged as key mediators of B cell dysfunction within the iCCA TME. Functional coculture experiments confirmed that

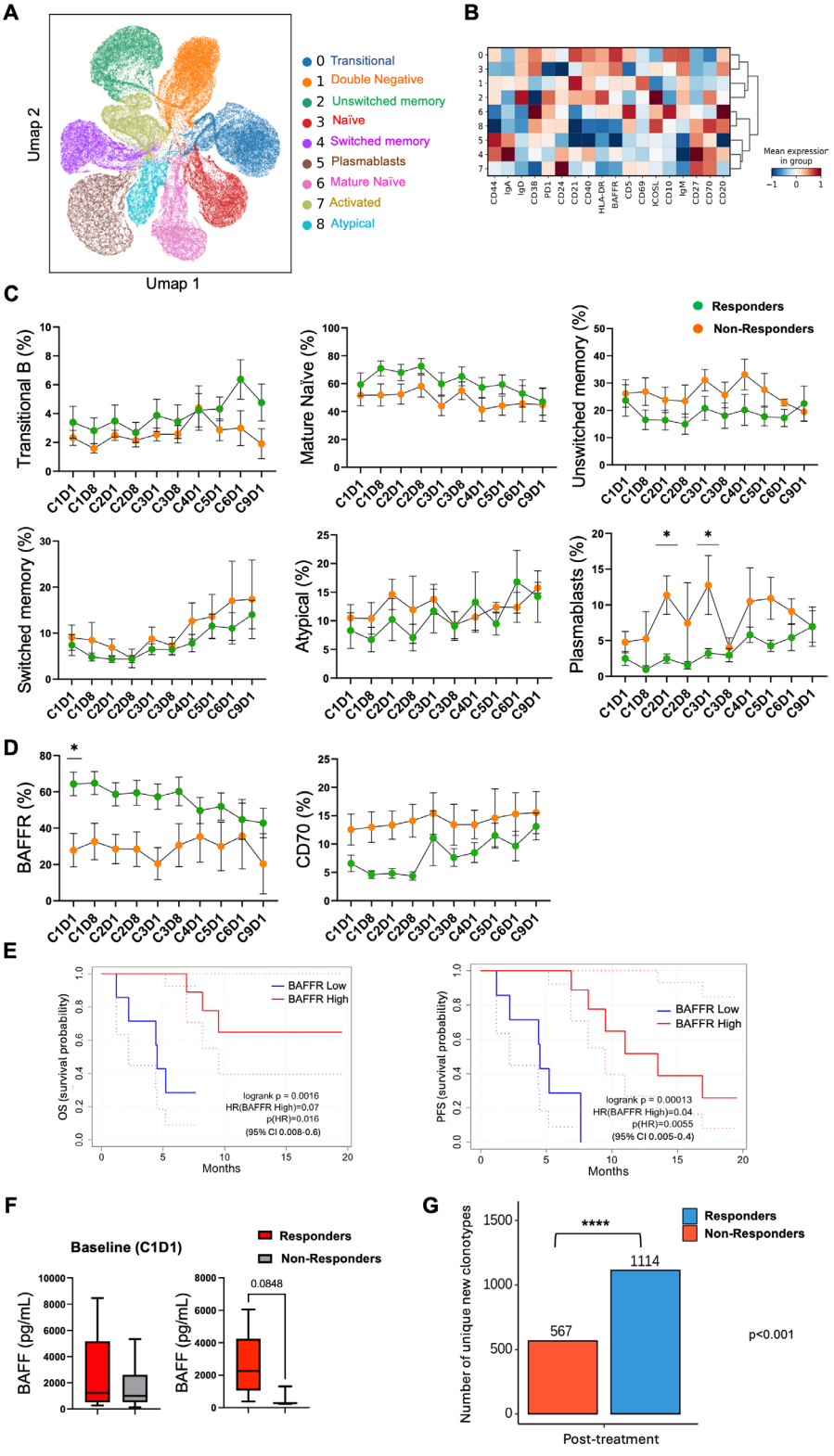

Figure 6 Circulating B cell phenotypes and clonal dynamics associate with clinical response to chemoimmunotherapy in iCCA. (A) UMAP representation of PhenoGraph clustering of peripheral CD19$^+$ B cells from iCCA patients (n=21), based on multiparametric flow cytometry. (B) Heatmap showing z-score normalised expression of selected activation and differentiation markers across identified B cell clusters. (C) Frequencies of circulating B cell subsets in responder versus non-responder (NR) patients at 10 time points during treatment. (D) Percentage of total CD19$^+$ B cells expressing key surface markers associated with activation (eg, BAFFR), maturation (eg, CD27) and exhaustion (eg, CD70). Error bars represent SD. Statistical analysis was performed using ANOVA. *p<0.05; ****p<0.0001. (E) Kaplan-Meier survival curves showing overall survival (OS), (E) and progression-free survival (PFS), (F) in patients with high versus low BAFFR expression on circulating B cells at baseline (n=21). (F) Quantification of soluble BAFF levels in plasma from responder and NR patients at baseline (cycle 1, day 1–C1D1) and at the end of treatment (C9D1), measured by ELISA. (G) Relationship between treatment-emergent shared hyperexpanded B cell clonotypes (defined by CDR3 amino acid sequence overlap) and clinical response to chemo-immunotherapy, assessed via $\chi 2$ test (p≤0.05). ANOVA, analysis of variance; iCCA, intrahepatic cholangiocarcinoma.

blocking TGF-β and IL-6R signalling restores B cell activation and differentiation. Notably, IL-6R inhibition disrupted inflammatory signals driving regulatory phenotypes, while combined inhibition promoted a more mature and pro-inflammatory B cell profile, with therapeutic implications.[60]

We also explored TLS formation, typically associated with antitumour immunity.[30 61] In iCCA, TLSs were generally scarce and, when present within tumours, were functionally ineffective and associated with poor outcomes,[53] likely due to immune exhaustion and the presence of suppressive subsets such as Tregs and exhausted B cells.[61 62] Conversely, peritumoural TLS correlated with higher B cell frequencies and were associated with late recurrence. These findings suggest that the absence of mTLS with functional germinal centres may hinder affinity maturation and memory B cell development, limiting antitumour efficacy. Promoting intratumoural mTLS may thus help overcome iCCA's immunosuppressive TME and contribute to improved patient outcomes. Induction of mTLS has been shown in other tumour types to support local antigen presentation, B cell maturation and the generation of tumour-specific immune responses, thereby enhancing sensitivity to ICIs. This scenario is reminiscent of observations in early-stage hepatocellular carcinoma.[54] A recent study by Ding *et al*[29] also reported a positive prognostic impact of intratumoural TLS in iCCA. However, their analysis included total TLS structures encompassing multiple immune cell types, without discriminating B cell phenotype or functionality. In contrast, our study specifically focuses on B cell composition and activation state within TLS and reveals that intratumoural TLS lacking mature, functional B cells may fail to support effective immune responses. Therefore, our findings complement and refine those of Ding *et al*,[29] suggesting that not only the presence but also the spatial distribution and immune quality of TLS, particularly the phenotypic and functional characteristics of B cells, may critically influence their clinical relevance in iCCA.

There is evidence that B cells and TLS in the TME are linked to ICI treatment response.[63] However, reliable predictive biomarkers for ICI efficacy in iCCA remain elusive. In this study, we prospectively assessed peripheral B-cell subsets in patients undergoing ICI-based therapy, evaluating both their predictive potential and dynamic changes over time. Responders showed a higher frequency of BAFFR$^+$ B cells, an activation marker associated with improved PFS and overall survival, and the emergence of hyperexpanded clonotypes, suggestive of therapy-induced clonal selection. In contrast, NR exhibited reduced activation, alongside increased CD70 expression, a marker of immune exhaustion and tumour progression, potentially contributing to therapeutic resistance.[49] These findings indicate that chemoimmunotherapy actively reshapes the B-cell repertoire and supports a dual role for B cells as both biomarkers and functional mediators of antitumour immunity.

Beyond underscoring the immunosuppressive nature of tumour-infiltrating B cells in iCCA, our results suggest that their phenotypic and functional profiles may influence, and potentially predict, clinical responses to immunotherapy. BAFFR$^+$ B cells, TLS maturity and IL-6R or TGF-β pathway inhibition may represent rational targets for patient stratification and therapeutic intervention. While our study offers novel insights into B cell dysregulation in iCCA, limitations should be acknowledged. While the low frequency of intratumoural B cells limited certain spatial and subset-specific analyses, and some assays relied on peripheral B cells from HDs, the consistency across phenotypic, transcriptomic and functional datasets reinforces the validity of our conclusions.

From a translational perspective, B cells emerge as both promising biomarkers and therapeutic targets in iCCA. Strategies aimed at restoring B-cell function, via cytokine blockade, enhancement of antigen presentation or induction of mTLS, could help reprogram the TME and improve immunotherapeutic efficacy. Notably, a recent study showed that VEGF inhibition promotes BAFF expression and TLS formation, further supporting the therapeutic relevance of targeting the BAFF axis to boost B cell–driven antitumour immunity.[64] Future clinical trials should evaluate combination approaches integrating B cell-modulating agents with ICIs to convert iCCA into a more immunologically responsive malignancy.

Author affiliations
[1]Hepatobiliary Immunopathology Lab, Department of Gastroenterology, IRCCS Humanitas Research Hospital, Rozzano (MI), Italy
[2]Flow Cytometry Core, IRCCS Humanitas Research Hospital, Rozzano (MI), Italy
[3]Institute of Genetic and Biomedical Research, UoS Milan, National Research Council, Rozzano, (MI), Italy
[4]Laboratory of Translational Immunology, IRCCS Humanitas Research Hospital, Rozzano (MI), Italy
[5]Division of Hepatobiliary and General Surgery, Department of Surgery, IRCCS Humanitas Research Hospital, Rozzano (MI), Italy
[6]Department of Biomedical Sciences, Humanitas University, Pieve Emanuele (MI), Italy
[7]Clinical Bioinformatics Unit, IRCCS Istituto Giannina Gaslini, Genoa, Italy
[8]Bioinformatics Unit, IRCCS Humanitas Research Hospital, Rozzano (MI), Italy
[9]Unit of Multiscale and Nanostructural Imaging, IRCCS Humanitas Research Hospital, Rozzano (MI), Italy
[10]Department of Experimental and Clinical Medicine, Università degli Studi di Firenze, Florence, Italy
[11]Division of Internal Medicine and Hepatology, Department of Gastroenterology, IRCCS Humanitas Research Hospital, Rozzano (MI), Italy
[12]Medical Oncology and Hematology Unit, Humanitas Cancer Center, IRCCS Humanitas Research Hospital, Rozzano (MI), Italy
[13]Pathology Unit, IRCCS Humanitas Research Hospital, Rozzano (MI), Italy
[14]Department of Medical Biotechnologies and Translational Medicine, Università degli Studi di Milano, Milan, Italy
[15]Immunity and Immunodeficiency Lab, IRCCS Humanitas Research Hospital, Rozzano (MI), Italy

Acknowledgements The authors wish to thank all the patients who participated in this study.

Contributors Conceptualisation and design of the study (GM, CC, SPu, PU, RC, EL, BC and AL). Data generation (GM, BF, GC, SPu, PU, DC, RC, GL-Z, IMa and ME). Patient selection and treatment (RB, TP, GC, GT and LR). Sample collection and processing (GM, BF, CS, MAP and GL-Z). Single-cell data analysis (SPi, PU, DC, RC, LL and AC). Data analysis and interpretation (GM, GC, SPi, PU, DC, RC, BC, EL and AL). Manuscript preparation (GM, BC, EL and AL). Critical review and paper editing (all authors). Funding (GM and AL). Guarantor: AL.

Funding This work was funded by the Associazione Italiana per la Ricerca sul Cancro (AIRC IG 2019–ID 23408 to AL). GM was supported by Italy Pre-doc Fellowships from the Associazione Italiana per la Ricerca sul Cancro (AIRC borsa di studio Italy Pre-Doc 2022–ID 28531).

Competing interests AL has received consulting fees from Advanz Pharma, GSK, Ipsen, Gilead, Dr Falk, AlfaSigma and Takeda, speaker fees from Gilead, AbbVie, MSD, Advanz Pharma, AlfaSigma, GSK, AstraZeneca, Ipsen and Incyte. She has received travel support from Ipsen and Falk Foundation and grant support (to Humanitas Research Hospital) from Mirum, GSK, Ipsen, Dr Falk, Gilead. LR has received consulting fees from AbbVie, AstraZeneca, Basilea, Bayer, BMS, Eisai, Elevar Therapeutics, Exelixis, Genenta, Hengrui, Incyte, Ipsen, IQVIA, Jazz Pharmaceuticals, MSD, Nerviano Medical Sciences, Roche, Servier, Taiho Oncology, Zymeworks; speaker fees from AstraZeneca, Bayer, BMS, Guerbet, Incyte, Ipsen, Roche, Servier; travel expenses from AstraZeneca; research funding to Humanitas Research Hospital from AbbVie, Agios, AstraZeneca, BeiGene, Eisai, Exelixis, Fibrogen, Incyte, Ipsen, Jazz Pharmaceuticals, Lilly, MSD, Nerviano Medical Sciences, Roche, Servier, Taiho Oncology, TransThera Sciences, Zymeworks. TP received/reports consulting fees from Bayer, Ipsen and AstraZeneca; institutional research funding from Roche, Bayer, AstraZeneca; support for congress attendance from Roche. EL is listed as the inventor on a patent on TSCM cells and received royalties related to that patent, received research funding from Bristol Myers Squibb on a topic unrelated to this paper and reports consulting fees from BD Biosciences, BioLegend, Swarm Oncology, Pfizer, Menarini and AstraZeneca. All the other authors have nothing to declare.

Patient and public involvement Patients and/or the public were not involved in the design, or conduct, or reporting, or dissemination plans of this research.

Patient consent for publication Consent obtained directly from patient(s).

Ethics approval The study, approved by the Humanitas Research Hospital Institutional Review Board (approval nos. 146/20 and 28/01/2016), was conducted in accordance with the Declaration of Helsinki. All participants provided informed consent.

Provenance and peer review Not commissioned; externally peer reviewed.

Data availability statement Data are available in a public, open access repository. Data are available on reasonable request. scRNA-seq data: raw data set is available in the Gene Expression Omnibus (GEO) database (http://www.ncbi.nlm.nih.gov/geo) under accession number GSE171899. Raw sc scRNA-seq and WES data were downloaded from the National Genomics Data Center after authorised access (accession number HRA000863). Data from: Song G et al. Single-cell transcriptomic analysis suggests two molecularly distinct subtypes of intrahepatic cholangiocarcinoma. Nat Commun. 2022 Mar 28;13:1642. doi: 10.1038/s41467-022-29164-0- Tables summarising clinical data are included. Scripts used to analyse the flow cytometry single-cell data are available at https://github.com/luglilab/Cytophenograph. All other codes are available on reasonable request.

Supplemental material This content has been supplied by the author(s). It has not been vetted by BMJ Publishing Group Limited (BMJ) and may not have been peer-reviewed. Any opinions or recommendations discussed are solely those of the author(s) and are not endorsed by BMJ. BMJ disclaims all liability and responsibility arising from any reliance placed on the content. Where the content includes any translated material, BMJ does not warrant the accuracy and reliability of the translations (including but not limited to local regulations, clinical guidelines, terminology, drug names and drug dosages), and is not responsible for any error and/or omissions arising from translation and adaptation or otherwise.

ORCID iDs
Luca Lambroia http://orcid.org/0000-0002-8724-1485
Ana Lleo http://orcid.org/0000-0002-0561-7902

REFERENCES

1 Oh D-Y, Ruth He A, Qin S, *et al*. Durvalumab plus Gemcitabine and Cisplatin in Advanced Biliary Tract Cancer. *NEJM Evid* 2022;1:EVIDoa2200015.
2 Kelley RK, Ueno M, Yoo C, *et al*. Pembrolizumab in combination with gemcitabine and cisplatin compared with gemcitabine and cisplatin alone for patients with advanced biliary tract cancer. *HAL Open Sci* 2024.:61.
3 Affo S, Filliol A, Gores GJ, *et al*. Fibroblasts in liver cancer: functions and therapeutic translation. *Lancet Gastroenterol Hepatol* 2023;8:748–59.
4 Zhou Z, Wang P, Sun R, *et al*. Tumor-associated neutrophils and macrophages interaction contributes to intrahepatic cholangiocarcinoma progression by activating STAT3. *J Immunother Cancer* 2021;9:1–12.
5 Liu D, Heij LR, Czigany Z, *et al*. The role of tumor-infiltrating lymphocytes in cholangiocarcinoma. *J Exp Clin Cancer Res* 2022;41:1–18.
6 Ma L, Hernandez MO, Zhao Y, *et al*. Tumor Cell Biodiversity Drives Microenvironmental Reprogramming in Liver Cancer. *Cancer Cell* 2019;36:418–30.
7 Vigano L, Soldani C, Franceschini B, *et al*. Tumor-Infiltrating Lymphocytes and Macrophages in Intrahepatic Cholangiocellular Carcinoma. Impact on Prognosis after Complete Surgery. *J Gastrointest Surg* 2019;23:2216–24.
8 Alvisi G, Termanini A, Soldani C, *et al*. Multimodal single-cell profiling of intrahepatic cholangiocarcinoma defines hyperactivated Tregs as a potential therapeutic target. *J Hepatol* 2022;77:1359–72.
9 Martin-Serrano MA, Kepecs B, Torres-Martin M, *et al*. Novel microenvironment-based classification of intrahepatic cholangiocarcinoma with therapeutic implications. *Gut* 2023;72:736–48.
10 Komai T, Inoue M, Okamura T, *et al*. Transforming Growth Factor-β and Interleukin-10 Synergistically Regulate Humoral Immunity *via* Modulating Metabolic Signals. *Front Immunol* 2018;9:1364.
11 Zhang E, Ding C, Li S, *et al*. Roles and mechanisms of tumour-infiltrating B cells in human cancer: a new force in immunotherapy. *Biomark Res* 2023;11:28.
12 Carsetti R, Terreri S, Conti MG, *et al*. Comprehensive phenotyping of human peripheral blood B lymphocytes in healthy conditions. *Cytometry Pt A* 2022;101:131–9.
13 Ramos RN, Amano MT, Paes Leme AF, *et al*. Editorial: Tumor microenvironment (TME) and tumor immune microenvironment (TIME): New perspectives for prognosis and therapy. *Front Cell Dev Biol* 2022;10:971275.
14 Flores-Borja F, Blair P. Mechanisms of induction of regulatory B cells in the tumour microenvironment and their contribution to immunosuppression and pro-tumour responses. *Clin Exp Immunol* 2022;209:33–45.
15 Xue VW, Chung J-F, Córdoba CAG, *et al*. Transforming Growth Factor-β: A Multifunctional Regulator of Cancer Immunity. *Cancers (Basel)* 2020;12:1–32.
16 Largeot A, Pagano G, Gonder S, *et al*. The B-side of Cancer Immunity: The Underrated Tune. *Cells* 2019;8:449:1–20:.
17 Yang Y-L, Yang F, Huang Z-Q, *et al*. T cells, NK cells, and tumor-associated macrophages in cancer immunotherapy and the current state of the art of drug delivery systems. *Front Immunol* 2023;14:1199173.
18 Fridman WH, Petitprez F, Meylan M, *et al*. B cells and cancer: To B or not to B? *J Exp Med* 2021;218:1–11.
19 Zhao Z, Ding H, Lin Z-B, *et al*. Relationship between Tertiary Lymphoid Structure and the Prognosis and Clinicopathologic Characteristics in Solid Tumors. *Int J Med Sci* 2021;18:2327–38.
20 Zhao L, Jin S, Wang S, *et al*. Tertiary lymphoid structures in diseases: immune mechanisms and therapeutic advances. *Signal Transduct Target Ther* 2024;9:225.
21 Laumont CM, Banville AC, Gilardi M, *et al*. Tumour-infiltrating B cells: immunological mechanisms, clinical impact and therapeutic opportunities. *Nat Rev Cancer* 2022;22:414–30.
22 Ma X, Bellomo L, Magee K, *et al*. Characterization of a Real-World Response Variable and Comparison with RECIST-Based Response Rates from Clinical Trials in Advanced NSCLC. *Adv Ther* 2021;38:1843–59.
23 Primavesi F, Fadinger N, Biggel S, *et al*. Early response evaluation during preoperative chemotherapy for colorectal liver metastases: Combined size and morphology-based criteria predict pathological response and survival after resection. *J Surg Oncol* 2020;121:382–91.
24 Clavarino G, Delouche N, Vettier C, *et al*. Novel Strategy for Phenotypic Characterization of Human B Lymphocytes from Precursors to Effector Cells by Flow Cytometry. *PLoS ONE* 2016;11:e0162209.
25 Kaur I, Vasudevan A, Rawal P, *et al*. Primary Hepatocyte Isolation and Cultures: Technical Aspects, Challenges and Advancements. *Bioengineering (Basel)* 2023;10:131.
26 Ribot JC, Serre K, Silva-Santos B. Developmental and Functional Assays to Study Murine and Human γδ T Cells. *Methods Mol Biol* 2017;1514:257–67.
27 Brummelman J, Haftmann C, Núñez NG, *et al*. Development, application and computational analysis of high-dimensional fluorescent antibody panels for single-cell flow cytometry. *Nat Protoc* 2019;14:1946–69.
28 Chen Y, Wu Y, Yan G, *et al*. Tertiary lymphoid structures in cancer: maturation and induction. *Front Immunol* 2024;15:1–13.
29 Ding G-Y, Ma J-Q, Yun J-P, *et al*. Distribution and density of tertiary lymphoid structures predict clinical outcome in intrahepatic cholangiocarcinoma. *J Hepatol* 2022;76:608–18.
30 Liang H, Zhang Z, Guan Z, *et al*. Follicle-like tertiary lymphoid structures: A potential biomarker for prognosis and immunotherapy response in patients with laryngeal squamous cell carcinoma. *Front Immunol* 2023;14:1–12.
31 Lynch KT, Young SJ, Meneveau MO, *et al*. Heterogeneity in tertiary lymphoid structure B-cells correlates with patient survival in metastatic melanoma. *J Immunother Cancer* 2021;9:e002273.
32 Morgan D, Tergaonkar V. Unraveling B cell trajectories at single cell resolution. *Trends Immunol* 2022;43:210–29.
33 Monaco G, Lee B, Xu W, *et al*. RNA-Seq Signatures Normalized by mRNA Abundance Allow Absolute Deconvolution of Human Immune Cell Types. *Cell Rep* 2019;26:1627–40.
34 Puccio S, Grillo G, Alvisi G, *et al*. CRUSTY: a versatile web platform for the rapid analysis and visualization of high-dimensional flow cytometry data. *Nat Commun* 2023;14:5102.
35 Pedersen CB, Dam SH, Barnkob MB, *et al*. cyCombine allows for robust integration of single-cell cytometry datasets within and across technologies. *Nat Commun* 2022;13:1698.
36 Centuori SM, Gomes CJ, Kim SS, *et al*. Double-negative (CD27−IgD−) B cells are expanded in NSCLC and inversely correlate with affinity-matured B cell populations. *J Transl Med* 2018;16:1–8.
37 Damelang T, de Taeye SW, Rentenaar R, *et al*. The Influence of Human IgG Subclass and Allotype on Complement Activation. *J Immunol* 2023;211:1725–35.
38 Laha D, Grant R, Mishra P, *et al*. The Role of Tumor Necrosis Factor in Manipulating the Immunological Response of Tumor Microenvironment. *Front Immunol* 2021;12:656908.
39 Song G, Shi Y, Meng L, *et al*. Single-cell transcriptomic analysis suggests two molecularly subtypes of intrahepatic cholangiocarcinoma. *Nat Commun* 2022;13:1642.
40 Zhang M, Yang H, Wan L, *et al*. Single-cell transcriptomic architecture and intercellular crosstalk of human intrahepatic cholangiocarcinoma. *J Hepatol* 2020;73:1118–30.
41 Feng X, Sun R, Lee M, *et al*. Cell circuits between leukemic cells and mesenchymal stem cells block lymphopoiesis by activating lymphotoxin beta receptor signaling. *Elife* 2023;12:1–18.
42 David K, Friedlander G, Pellegrino B, *et al*. CD74 as a regulator of transcription in normal B cells. *Cell Rep* 2022;41:111572.

43 Huai G, Markmann JF, Deng S, *et al*. TGF-β-secreting regulatory B cells: unsung players in immune regulation. *Clin & Trans Imm* 2021;10:1–14.
44 Zhang H, Wen H, Zhu Q, *et al*. Genomic profiling and associated B cell lineages delineate the efficacy of neoadjuvant anti-PD-1-based therapy in oesophageal squamous cell carcinoma. *EBioMedicine* 2024;100:104971.
45 Smith LK, Fawaz K, Treanor B. Galectin-9 regulates the threshold of B cell activation and autoimmunity. *Elife* 2021;10:1–29.
46 Zhao Z, Li T, Sun L, *et al*. Potential mechanisms of cancer-associated fibroblasts in therapeutic resistance. *Biomed Pharmacother* 2023;166:115425.
47 Administration F and D. FDA approves durvalumab for locally advanced or metastatic biliary tract cancer. 2008.282.
48 Guo FF, Cui JW. The Role of Tumor-Infiltrating B Cells in Tumor Immunity. *J Oncol* 2019;2019:2592419.
49 Flieswasser T, Van den Eynde A, Van Audenaerde J, *et al*. The CD70-CD27 axis in oncology: the new kids on the block. *J Exp Clin Cancer Res* 2022;41:12.
50 Smulski CR, Eibel H. BAFF and BAFF-Receptor in B Cell Selection and Survival. *Front Immunol* 2018;9:2285.
51 Gierlikowska B, Stachura A, Gierlikowski W, *et al*. Phagocytosis, Degranulation and Extracellular Traps Release by Neutrophils—The Current Knowledge, Pharmacological Modulation and Future Prospects. *Front Pharmacol* 2021;12:1–21.
52 Chang HD, Radbruch A. Maintenance of quiescent immune memory in the bone marrow. *Eur J Immunol* 2021;51:1592–601.
53 Zhang H, AbdulJabbar K, Moore DA, *et al*. Spatial Positioning of Immune Hotspots Reflects the Interplay between B and T Cells in Lung Squamous Cell Carcinoma. *Cancer Res* 2023;83:1410–25.
54 Meylan M, Petitprez F, Lacroix L, *et al*. Early Hepatic Lesions Display Immature Tertiary Lymphoid Structures and Show Elevated Expression of Immune Inhibitory and Immunosuppressive Molecules. *Clin Cancer Res* 2020;26:4381–9.
55 Sachinidis A, Garyfallos A. Double Negative (DN) B cells: A connecting bridge between rheumatic diseases and COVID-19? *Mediterr J Rheumatol* 2021;32:192–9.
56 Wojtukiewicz MZ, Rek MM, Karpowicz K, *et al*. Inhibitors of immune checkpoints-PD-1, PD-L1, CTLA-4-new opportunities for cancer patients and a new challenge for internists and general practitioners. *Cancer Metastasis Rev* 2021;40:949–82.
57 Luo W, Weisel F, Shlomchik MJ. B Cell Receptor and CD40 Signaling Are Rewired for Synergistic Induction of the c-Myc Transcription Factor in Germinal Center B Cells. *Immunity* 2018;48:313–26.
58 Sarvaria A, Madrigal JA, Saudemont A. B cell regulation in cancer and anti-tumor immunity. *Cell Mol Immunol* 2017;14:662–74.
59 Moreira H, Dobosz A, Cwynar-Zając Ł, *et al*. Unraveling the role of Breg cells in digestive tract cancer and infectious immunity. *Front Immunol* 2022;13:981847.
60 Perez-Penco M, Byrdal M, Lara de la Torre L, *et al*. The antitumor activity of TGFβ-specific T cells is dependent on IL-6 signaling. *Cell Mol Immunol* 2025;22:111–26.
61 Fridman WH, Meylan M, Pupier G, *et al*. Tertiary lymphoid structures and B cells: An intratumoral immunity cycle. *Immunity* 2023;56:2254–69.
62 Daniel L, Bhattacharyya ND, Counoupas C, *et al*. Stromal structure remodeling by B lymphocytes limits T cell activation in lymph nodes of Mycobacterium tuberculosis-infected mice. *J Clin Invest* 2022;132:e157873.
63 Author BAH, Woodman SZK. B cells and tertiary lymphoid structures promote immunotherapy response. *Nature New Biol* 2020;577:549–55.
64 Benmebarek M-R, Oguz C, Seifert M, *et al*. Anti-vascular endothelial growth factor treatment potentiates immune checkpoint blockade through a BAFF- and IL-12-dependent reprogramming of the TME. *Immunity* 2025;58:926–45.